Chemistry & Biology, Vol. 11, 517–524, April, 2004, ©2004 Elsevier Science Ltd. All rights reserved. DOI 10.1016/j.chembiol.2004.03.020

Simultaneous Characterization of the Reductive Unfolding Pathways of RNase B Isoforms by Top-Down Mass Spectrometry

Guoqiang Xu, Huili Zhai, Mahesh Narayan, Fred W. McLafferty, and Harold A. Scheraga*
Baker Laboratory of Chemistry and Chemical Biology
Cornell University
Ithaca, New York 14853

Summary

A novel method for characterization of the simultaneous reductive unfolding pathways of five isoforms of bovine pancreatic ribonuclease B (RNase B) is demonstrated. The results indicate that each isoform unfolds reductively through two three-disulfide-containing structured intermediates before proceeding to the fully reduced form, as in the reductive unfolding pathways of the A variant lacking the carbohydrate chain. The rates of reduction of bovine pancreatic ribonuclease A (RNase A) and RNase B and the formation and consumption of their reductive intermediates are identical, indicating that the unfolding events necessary to expose disulfide bonds for reduction are not affected by the oligosaccharide. The method utilizes top-down mass spectrometry and a naturally occurring tag on the protein, viz. the carbohydrate moiety, to obtain unfolding information of an ensemble of protein isoforms and is a generally applicable methodological advance for conducting folding studies on mixtures of different proteins.

Introduction

Glycosylation of proteins is a cotranslational event that usually involves the covalent modification of the Asn side chain(s) of the polypeptide by the attachment of a carbohydrate moiety [1–7]. Glycosylation can affect the physical properties of the proteins, provide lectin-recognition sites [2–4], and play an important role in transport, secretion of proteins, their anchoring to specific sites, and in protease protection [3]. Understanding the impact of glycosylation on protein folding/unfolding is important for understanding the aforementioned downstream processes.

Although a large amount of data exist on the impact of carbohydrate moieties on the folding and unfolding of proteins [8–16], a detailed understanding of the influence of glycosylation on the redox-dependent folding/unfolding pathways of multi-disulfide-containing proteins has not been undertaken and remains an important unanswered question, given that glycosylation is known to precede the folding process [1, 8, 9, 17].

Reductive unfolding, which is the conformational unfolding of the protein achieved by reducing its disulfide bonds, is a useful tool to study the unfolding pathways of multiple-disulfide-containing proteins [18–25]. Reductive unfolding experiments are helpful in understanding the nature of the unfolding event that is necessary to expose particular disulfide bonds, the impact of certain disulfide bonds on the native structure, the pathway(s) by which the protein unfolds, and the overall (global) stability of a protein.

Bovine pancreatic ribonuclease B (RNase B) [26], which constitutes ~15% of the total pancreatic ribonuclease [9] and occurs naturally as a mixture of five glycoforms (denoted as $Man_{5-9}GlcNAc_2$-RNase B) [27, 28], appears ideally suited as a model protein to understand the role of oligosaccharides in the reductive unfolding pathways of a protein. This is because its amino acid sequence is identical to that of RNase A (a well-studied protein [29–37]) and differs from the A variant by the presence of a single carbohydrate moiety attached to Asn 34 [26, 29]. Furthermore, a comparison of the crystal structures of the two variants [26, 29] reveals no significant differences, suggesting that the oligosaccharide moiety has no influence on the static conformation of the protein. The data obtained from redox-dependent folding/unfolding studies on RNase B can, therefore, easily be compared against a large amount of existing literature on the redox-dependent folding/unfolding of RNase A [22, 31, 33–37]. Furthermore, since RNase A cannot be glycosylated in its folded form [38], RNase B is, therefore, a good model system with which to study the influence of the carbohydrate group on the folding/unfolding pathway of bovine pancreatic ribonuclease.

Previous experiments showed that the kinetics of conformational unfolding and refolding of RNase A and B in GdnHCl are similar and proceed through a two-state mechanism [9], which indicates that the oligosaccharide has no significant effect on conformational folding under these conditions. However, the free energy of conformational unfolding of RNase B is greater than that of RNase A [9, 39]. Furthermore, measurements of amide-proton/deuterium exchange rates have suggested that the presence of the glycan affects the solvent accessibility of many regions of the peptide backbone in the vicinity of (e.g., residues 29–35), and at sites remote from (e.g., residues 57–61 and 75–76), the glycosylation site (Asn 34) [2, 4, 40]. Spatially, the glycosylation site is near the (40–95) disulfide bond [26], which is one of the first disulfide bonds [the other being the (65–72) disulfide bond] to be reduced in RNase A [22]]. Since reductive unfolding pathways and rates can be modulated by local protein fluctuations [22, 41], the effect of oligosaccharide on the reductive unfolding pathways and on the reductive unfolding rate of RNase B is the object of our study.

Protein folding and unfolding studies (both redox dependent and conformational) normally involve the acquisition of data arising from a single protein under various folding/unfolding conditions [18–25, 30–37, 42]. This is simply because it is very difficult to separate and analyze intermediates belonging to one protein species, let alone a mixture of species. In this article, we have stud-

*Correspondence: has5@cornell.edu

ied the simultaneous reductive unfolding of five isoforms of RNase B, a glycosylated form of RNase A, and characterized the reductive unfolding pathways of each isoform. This has been possible by the application of top-down mass spectrometry (MS) [43–47] to resolve the masses of each isoform and its reductive unfolding intermediates, for which purpose the carbohydrate moiety has served as a unique marker. Furthermore, the disulfide bonds that are reduced in the intermediates have been identified. This research has enabled us to gain insight into the role of the carbohydrate moiety in the reductive unfolding pathways of bovine pancreatic ribonuclease, and the significance and generality of the method is discussed.

Results

Purification of RNase B and Identification of Isoforms

Cation-exchange HPLC was used to remove any RNase A from commercial RNase B. ESI/FTMS analysis of the major peak in the cation-exchange chromatogram confirmed the absence of RNase A. All five isoforms of RNase B were detected by mass spectrometry (Figure 1A) and subsequently identified. Table 1 summarizes the relative molecular weight of each isoform and its identity.

Reductive Unfolding of RNase B and Identity of Reductive Intermediates

Reductive unfolding of RNase B was initiated by using using reduced dithiothreitol (DTT^{red}) (100 mM, pH 8, 15°C) and followed by electrospray ionization/Fourier-transform mass spectrometry (ESI/FTMS). Figures 1B and 1C are composites of an ESI/FTMS spectrum of the 2-aminoethylmethylthiosulfonate (AEMTS)-blocked reaction mixture 400 min after initiation of the reduction process. The fully reduced proteins are well resolved from the native protein isoforms and structured reductive intermediates (Figure 1B) because they have higher charge states due to their lack of rigid structure compared to structured species. The inset in Figure 1C shows the expanded portion of the spectrum in which the overlapping peaks of the native protein and its reductive intermediates are better resolved. The dots on the expanded portions represent the theoretical abundance distribution of the isotopic peaks. In addition to the five native isoforms of RNase B, which are partially overlapped with its intermediates, ten other peaks are clearly identifiable (see Figures 1B and 1C). The masses corresponding to each of these ten peaks indicate that, for each native isoform, its corresponding stable three-disulfide-containing intermediate (3S*) and fully reduced species (R) are formed. This analysis is easily accomplished because each AEMTS adduct leads to an increase in the molecular weight of the native protein by 76 Da [31]. Therefore, a three-disulfide-containing intermediate with its free thiols blocked by AEMTS will have a mass increase of 152 Da compared to the parent molecule. No other (one- or two-disulfide-containing) intermediates are observed for any of the isoforms, which is similar to that in the reduction of RNase A [22]. Sampling of the mixture at different reductive unfolding times gave the same results (except for a change in the relative abundance of the different species of each isoform). Therefore, our data indicate that reductive unfolding in each of the five isoforms of RNase B is initiated by the loss of one disulfide bond to form at least one three-disulfide-containing stable intermediate.

For a four-disulfide-containing protein, there can be four isomeric native three-disulfide-bond-containing intermediates having the same mass. We used cation-exchange HPLC to investigate the presence of multiple isomeric reductive intermediates that may be populated during the reductive unfolding of RNase B. Figure 2 shows typical HPLC chromatograms of the AEMTS-blocked reductive unfolding mixture of RNase B using DTT^{red} (100 mM, pH 8, 15°C) (Figure 2A, 202 min and Figure 2B, 1600 min after initiation of reductive unfolding). Four peaks are observed in each chromatogram. ESI/FTMS analysis of the separated peaks within each chromatogram indicated that the first peak contains all five isoforms of native RNase B (N); the peaks labeled I_1 and I_2 correspond to AEMTS-blocked three-disulfide-containing intermediates of all five isoforms of the protein, and the last peak contains all five isoforms of fully reduced protein (R) (Figure 2). This indicates that there are at least two three-disulfide-containing intermediates for RNase B. The fractional concentrations of N, I_1, I_2, and R are 0.777, 0.094, 0.039, and 0.090, respectively, at 202 min of reduction time and 0.356, 0.275, 0.130, and 0.239, respectively, 1600 min after initiation of reduction.

Identification of the Missing Disulfide Bonds in I_1 and I_2

A top-down mass spectrometry approach [46] was applied to determine the identity of the two free cysteines in each of the two intermediates, viz. I_1 and I_2. Linear molecules provide the most direct MS data interpretation, so the free cysteines were derivatized with iodoacetamide, then the remaining disulfide bonds were reduced and derivatized with AEMTS. Analysis of the derivatized intermediates I_1 and I_2 using ESI/FTMS indicated that the eight cysteines in all of the five RNase B isoforms were blocked by two iodoacetamide molecules and six AEMTS molecules, which is inferred from the agreement between the experimental molecular weight (M_{exp}) with the calculated molecular weight (M_{cal}) of the native proteins and two fully blocked intermediates (see Table 2). Blocking of one free thiol with an iodoacetamide molecule increases the molecular weight of the protein by 58 Da. Figure 3A shows the mass spectrum for the five isoforms of reduced AEMTS-blocked carboxymethylated I_1. All of the corresponding five isoforms were also observed for I_2 (data not shown). After ejection of all but the isoform I molecular ion of $Man_5GlcNAc_2$-RNase B (Figure 3A), infrared multiphoton dissociation (IRMPD) of the molecular ions resulted in 20 and 21 fragment ions (Figure 3B) that contain either the N-terminal ("***b*** ions") or the C-terminal ("***y*** ions") for I_1 and I_2, respectively. These fragments indicated that I_1 lacks the (65-72) disulfide bond and I_2 lacks the (40-95) disulfide bond, as discussed below.

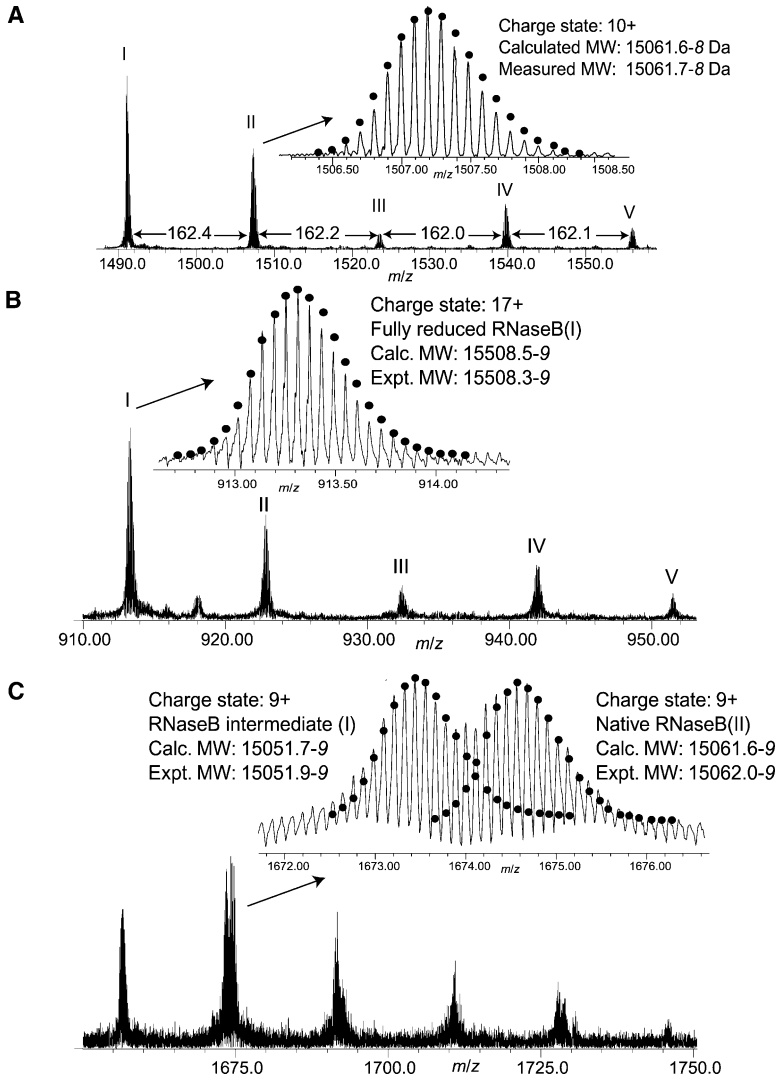

Figure 1. ESI/FTMS Spectra of RNase B and Its Reductive Intermediates

ESI/FTMS spectra of (A) native RNase B isoforms (the relative molecular weights of individual isoforms and the assignment of carbohydrate chains are listed in Table 1; the mass of a hexose unit is 162.2 Da), (B) reductive unfolding mixture of RNase B isoforms after 400 min reduction under 100 mM DTT^{red} (pH 8) and 15°C showing fully reduced RNase B, (C) a mixture of native (i.e., as yet unreduced) isoforms and their three-disulfide-containing reductive intermediates [same sample as (B)]. Dots on the expanded portions (insets) in each panel represent the theoretical abundance distribution of the isotopic peaks. The mass difference between the most abundant peak and the monoisotopic peak is denoted in italics. The inset in (C) shows the expanded version of the spectrum for one of the isoform peaks, indicating separation of the native isoform II from the three-disulfide-containing reductive intermediate of isoform I.

For I_1 (Figure 3C), the y_{20} fragment ion (the ion containing the last 20 amino acids) showed a mass increase of 75 Da compared to the sequence-derived value, indicating that Cys 110 was blocked by AEMTS instead of iodoacetamide. In a similar manner, y_{41} suggests that there were three AEMTS moieties in the last 41 amino acids, indicating that Cys 84 and Cys 95 were both blocked by AEMTS. Therefore, the (58-110), (26-84), and (40-95) disulfide bonds are the last to be reduced since they are blocked with AEMTS. This was confirmed by the complimentary b_{83} ion, which showed that there were three AEMTS additions and two alkylations in the first 83 amino acids, suggesting that Cys 65 and Cys 72 were blocked by iodoacetamide. According to the above analysis, it can be concluded that the reduced disulfide bond in I_1 is the (65-72) bond because the cysteines of the first reduced bond were alkylated by iodoacetamide, and thus I_1 is des [65-72] (a structured intermediate of RNase B having all native disulfide bonds but lacking the (65-72) disulfide bond).

For I_2 (data not shown), the b_{28} and y_{20} ions showed a mass increase of 75 Da, indicating that Cys 26 and Cys 110 were both blocked by AEMTS. The y_{41} fragment ion showed that there were one alkylation and two AEMTS

Table 1. Experimental Molecular Weight (M_{exp}) and Calculated Molecular Weight (M_{cal}) Values for the Isoforms of Native RNase B and the Assignment of the Carbohydrate Chain in Each Isoform

Peaks	M_{cal} (Da)	M_{exp} (Da)	Assignment of Carbohydrate Chain
I	14899.4	14899.3	$Man_5GlcNAc_2$
II	15061.6	15061.7	$Man_6GlcNAc_2$
III	15233.8	15223.9	$Man_7GlcNAc_2$
IV	15386.0	15385.9	$Man_8GlcNAc_2$
V	15548.2	15548.0	$Man_9GlcNAc_2$

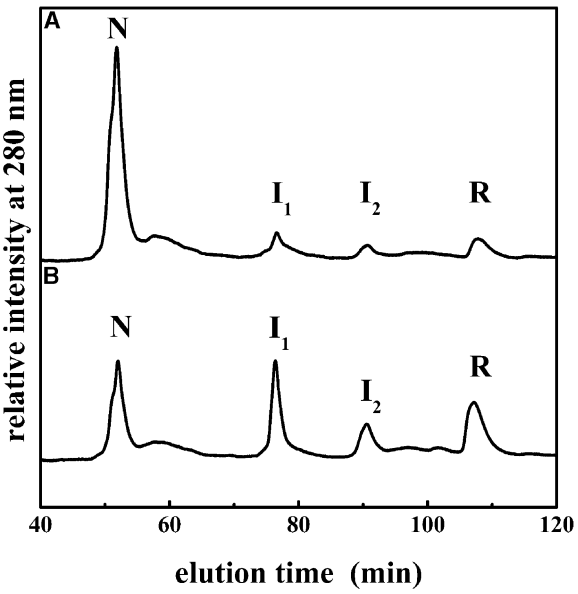

Figure 2. HPLC Chromatograms of the Reductive Unfolding of RNase B

Chromatograms at 202 min (A) and 1600 min (B) after initiation of the reductive unfolding of RNase B. Four peaks are observed in the chromatograms, N, I_1, I_2, and R. Experimental conditions are 1.0 mg/ml RNase B, 100 mM DTT^{red} (pH 8), and 15°C.

moieties in the last 41 amino acids, while the complimentary b_{83} ion suggests four AEMTS and one alkylation in the first 83 amino acids. Since disulfide-bond reshuffling is negligible under the alkylation conditions, which was confirmed by the absence of other alkylated sites in the mass spectra, it can be concluded that Cys 40 and Cys 95 were blocked by iodoacetamide, and thus that I_2 is des [40-95].

Fragmentation of the other isoforms in I_1 and I_2 gave the same results as isoform I, suggesting that the same disulfide bonds [i.e., (65-72) and (40-95)] were reduced in these two three-disulfide-containing intermediates for all of the RNase B isoforms. The disulfides of these two reductive unfolding intermediates in RNase B are the same as those of the intermediates in the reduction of wild-type RNase A [22].

Kinetics of the Reductive Unfolding of RNase B

Figure 4 shows the kinetics of reduction of RNase B (100 mM DTT^{red}, pH 8, 15°C) and the formation of its reductive unfolding intermediates (which is assessed by HPLC separation of AEMTS-blocked intermediates). The populations of I_1 and I_2 first increase and then decrease, indicating that they are eventually reduced after initially accumulating. There is a lag time in the formation of fully reduced protein (R), and it appears only after the formation of the three-disulfide-containing reductive intermediates, I_1 and I_2. Figure 4 also shows the reduction of native RNase A under the same condition (100 mM DTT^{red}, pH 8, 15°C).

Finally, we analyzed the fractions of des [65-72] and des [40-95] in the two variants (RNase A and B) formed as a function of reductive unfolding time (this is possible by comparing data in Figure 4 and those reported previously [22]) and found them to be similar for both variants (see the implications in the Discussion section).

Discussion

Reductive Unfolding Pathways of RNase B Using Top-Down MS

In this study, we have used a powerful analytical tool, viz. top-down MS, for a study of the simultaneous reductive unfolding pathways of multiple protein isoforms of RNase B. This has been accomplished by making use of the unsurpassed resolving power of ESI to differentiate between protein species having small mass differences and by utilizing the carbohydrate moiety, which is a natural marker attached to the protein, to distinguish one isoform from another. Traditional separation techniques such as HPLC would not be helpful in our study, since it is not possible (to our knowledge) to separate all of the protein isoforms and their reductive unfolding intermediates from one another in the simultaneous reductive unfolding pathways of RNase B. The different types of species in the mixture are the structurally similar five native isoforms, the native-like reductive unfolding intermediates of each isoform, and the fully reduced species of each isoform.

Our results indicate that the reductive unfolding of each of the five isoforms of RNase B takes place by reduction of one disulfide bond to produce a structured three-disulfide-containing intermediate. Mapping of the three-disulfide-containing intermediates in each isoform revealed that the (65-72) and the (40-95) disulfide bonds are the first to be reduced in parallel, to produce two three-disulfide-containing intermediates, viz. des [65-72] and des [40-95]. Each of these reductive intermedi-

Table 2. Experimental Molecular Weight (M_{exp}) and Calculated Molecular Weight (M_{cal}) Values of Reduced AEMTS-Blocked Carboxymethylated Intermediates I_1 and I_2

	Reduced AEMTS-Blocked Carboxymethylated I_1		Reduced AEMTS-Blocked Carboxymethylated I_2	
Isoforms of RNase B	M_{cal} (Da)	M_{exp} (Da)	M_{cal} (Da)	M_{exp} (Da)
I: $Man_5GlcNAc_2$	15472.3	15472.2	15472.3	15472.5
II: $Man_6GlcNAc_2$	15634.5	15634.7	15634.5	15634.8
III: $Man_7GlcNAc_2$	15796.7	15796.3	15796.7	15796.9
IV: $Man_8GlcNAc_2$	15958.9	15958.6	15958.9	15958.9
V: $Man_9GlcNAc_2$	16121.1	16121.0	16121.1	16120.9

The relative molecular weight increases by 58.05 Da and 76.13 Da when a thiol is blocked by one iodoacetamide and one AEMTS molecule, respectively.

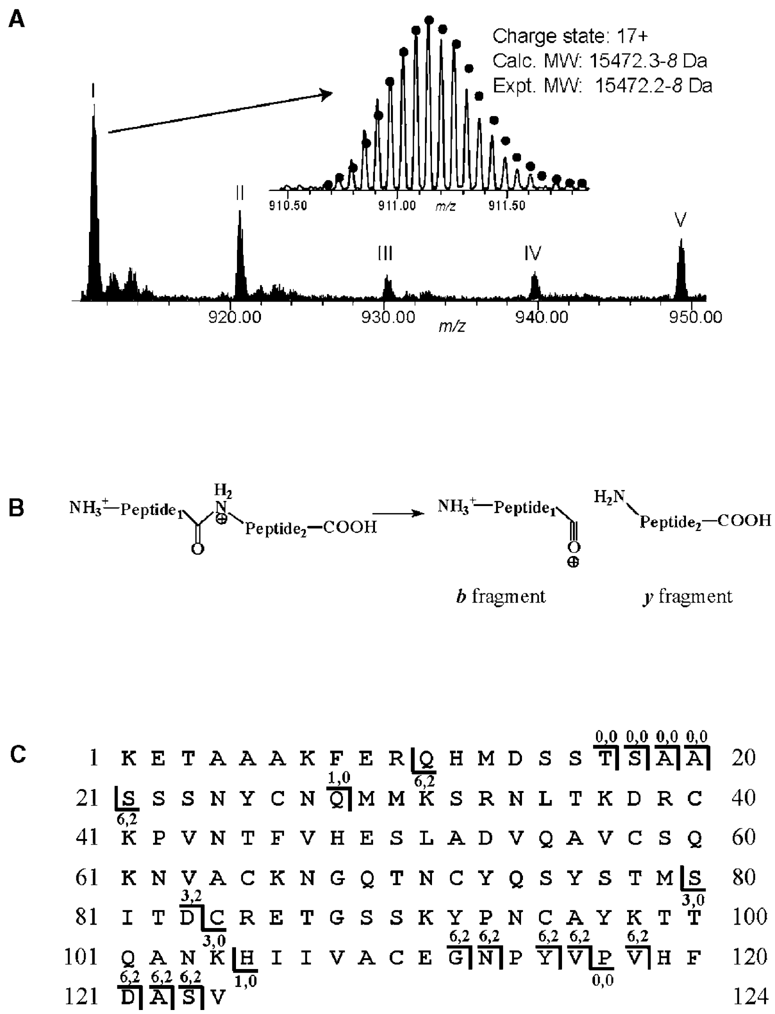

Figure 3. Mapping of RNase B Reductive Unfolding Intermediates

(A) ESI/FTMS spectrum of reduced AEMTS-blocked carboxymethylated reductive unfolding intermediate I_1. Dots on the expanded portions represent the theoretical abundance distribution of the isotopic peaks. The experimental and calculated molecular weights of individual isoforms are listed in Table 2. The mass difference between the most abundant peak and the monoisotopic peak is denoted in italics.

(B) The generation of the *b* (amino terminus) and *y* (carboxyl terminus) fragments observed with IRMPD. (C) The fragmentation map of I_1 (a three-disulfide-containing reductive intermediate of RNase B) obtained by IRMPD. The labeled fragments extend from the site of the cleavage (⌉ or ⌊) to either the amino or the carboxyl terminus of the protein. The numbers of cysteines that are covalently modified with AEMTS or iodoacetamide (separated by a comma) in the observed fragments are marked above or below the short horizontal segments for the amino (⌉) and carboxyl (⌊) terminus of the protein, respectively.

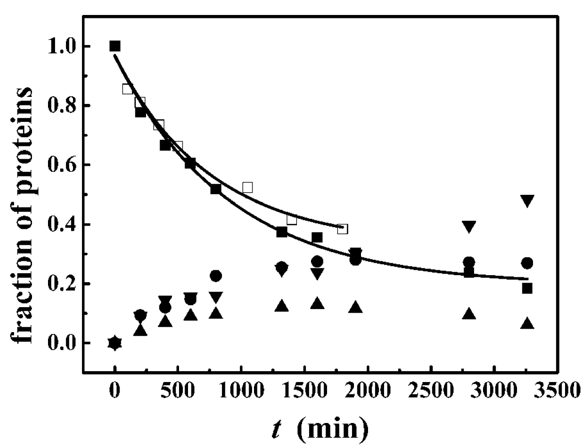

Figure 4. Kinetics of Reductive Unfolding of RNase B and RNase A

The fraction of RNase B species (N, ■; I_1, ●; I_2, ▲; R, ▼) and native RNase A (□) during the reductive unfolding under the same conditions (1.0 mg/ml protein, 100 mM DTT^{red} (pH 8), and 15°C). The solid curves are the single exponential fits.

ates in every isoform is then reduced to form the fully reduced protein (R) without populating any two- or one-disulfide-containing intermediates. The reductive unfolding pathways of RNase B are therefore identical to the reductive unfolding pathways of RNase A that lacks the carbohydrate moiety, as illustrated by Figure 5, with 2S being a postulated nondetectable intermediate.

The kinetics of reduction of RNase A (Figure 4a in reference [22]) and RNase B (Figure 4) are identical within experimental error, indicating that the reduction of the (65-72) disulfide bond in variant A and B takes place at the same rate. Similarly, the reductions of the

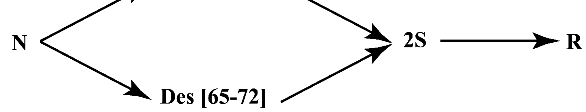

Figure 5. Reductive Unfolding Pathways of RNase B

The reductive unfolding of RNase B (N) takes place in two parallel pathways by reduction of the (40-95) and (65-72) disulfide bonds to form des [40-95] and des [65-72], respectively. These two reductive intermediates are then further reduced to form two-disulfide-containing intermediates (2S) and the fully reduced protein (R).

(40-95) disulfide bond in the two ribonuclease variants have the same rate under the same condition. However, since RNase B is a mixture of five isoforms which we did not separate, our data for its reduction represents an average rate that might actually be slightly different (although unlikely to be so) for each isoform.

Role of Oligosaccharides in the Reductive Unfolding of Bovine Pancreatic Ribonuclease

Our experiments were designed to gain an understanding of the role of a carbohydrate residue in protein unfolding. Bovine pancreatic ribonuclease serves as an excellent model system for this purpose for reasons previously mentioned in the Introduction. Our data indicate that the local fluctuations necessary for exposing the (40-95) and (65-72) disulfide bonds in the B variant, on average, are the same as in the A variant, and as a result the unfolding pathways and rates in both variants are identical (within experimental error). Therefore, the changes in the dynamics of the protein backbone that were previously observed in the B variant [2, 4, 40] are not sufficient to influence the local unfolding processes in the vicinity of the (40-95) and (65-72) disulfide bonds of the protein.

Furthermore, the fractional concentrations of des [65-72] and des [40-95] in the two variants, RNase A and RNase B, as a function of reductive unfolding time were similar (fractions of des [40-95] and des [65-72] for RNase B are shown in Figure 4 and those for RNase A are shown in Figure 4a in reference [22]), suggesting that the oligosaccharide moiety did not perturb the structure of the reductive unfolding intermediates of the B variant. Interestingly, initial results on the oxidative folding of RNase B indicate that its initial oxidative folding rate is ~1.5-fold faster than that of RNase A (unpublished observation).

Significance

The significance of our study is two-fold.

We have demonstrated that the reductive unfolding of all five isoforms of RNase B is initiated by the loss of one disulfide bond to form two stable three-disulfide-containing intermediates, des [65-72] and des [40-95], before forming the fully reduced protein (R) and is therefore similar to the reductive unfolding pathways of RNase A, which lacks the carbohydrate moiety. These data indicate that the local unfolding processes that are required to expose the (65-72) and (40-95) disulfide bonds in RNase B are unaffected by any dynamic fluctuations induced by the presence of the carbohydrate moiety.

The complex nature of redox-dependent protein folding/unfolding pathways has previously necessitated the study of a single protein species at a time. In such studies, HPLC fractionation of the intermediates is achieved, followed by the determination of the identity of each intermediate, carried out by assessing its molecular weight using mass spectrometry. In this study, we have used a powerful analytical tool, viz. top-down MS, to characterize the simultaneous reductive unfolding pathways of five isoforms of the glycoprotein, RNase B. Here, not only is the oligosaccharide moiety the subject of our study, but it has also served as an analytical handle for differentiating between the five isoforms of RNase B and their reductive unfolding intermediates. To our knowledge, there is no previous report of such a detailed understanding of reductive unfolding of a mixture of protein isoforms.

The approach developed here can possibly be used to study a more complex system of macromolecules and, in the future, may be useful to study protein folding/unfolding in crude cell extracts.

Experimental Procedures

Materials

RNase B was purchased from Sigma and purified by use of a strong cation-exchange (SCX) HPLC (Rainin Hydropore 5-SCX column) system. Two buffers were used for the purification process. Buffer A contained 25 mM HEPES and 1 mM EDTA at pH 7, and buffer B consisted of buffer A plus 1 M sodium chloride. A linear gradient of buffer B from 1 to 3% (buffer A from 99 to 97%) was used within 60 min to separate the two variants. The molecular weights of the individual isoforms of RNase B were determined by ESI/FTMS, and the compositions of the isoforms were assigned. AEMTS (above 99% purity) was purchased from Anatrace. Iodoacetamide and reduced dithiothreitol were obtained from Sigma and used without further purification. All other chemicals were of the highest grade commercially available.

Reductive Unfolding of RNase B

Purified RNase B was dissolved in a pH 3 acetic acid buffer (10 mM) to obtain a stock solution (5.0 mg/ml). Reductive unfolding of RNase B was initiated by introducing 0.2 ml of the protein stock solution into 0.8 ml of a pH 8.0 buffer containing DTT^{red} at 15°C. The final reaction solution contained 100 mM DTT^{red} (50 mM Tris-HCl, 1 mM EDTA), and the concentration of RNase B was 1.0 mg/ml. The reaction mixture was continuously sparged with argon during the experiment. Aliquots of 100 μl were withdrawn at different times, and the free thiols in each aliquot were blocked with an excess amount of AEMTS. After 5 min, the pH of the AEMTS-blocked samples was reduced to 3 by the addition of 20 μl glacial acetic acid. This procedure prevents deamidation [48]. The samples were then desalted and lyophilized.

Mass Spectrometric Analysis of the Reductive Unfolding Pathways of RNase B

The AEMTS-blocked lyophilized samples described above were subjected to mass spectrometric analysis. For this purpose, the samples were dissolved in 50:48:2 (H_2O:CH_3OH:CH_3COOH) solution and electrosprayed at 1-50 nl/min with a nanospray emitter. Mass spectra were acquired on a 6 T modified Finnigan FTMS described previously [43]. Fragmentation was achieved by infrared multiphoton dissociation (IRMPD) and sustained off-resonance irradiation collisionally activated dissociation (CAD) [44]. The MS/MS spectra are averages of 20–100 scans. Assignments of the fragment masses and compositions were made with the computer program THRASH [45]. After each mass value, the mass difference (in unit of 1.00235 Da) between the most abundant isotopic peak and the monoisotopic peak is denoted in italics (as seen in Figures 1 and 3A).

Determination of Multiple Isomeric Intermediates in the Reductive Unfolding Pathway of RNase B

In order to check for multiple isomeric intermediates (indistinguishable by mass spectrometry), HPLC separation was attempted. In RNase A, the isomeric des [40-95] and des [65-72] can be successfully separated from one another using cation-exchange HPLC [22].

Reductive unfolding of RNase B was carried out as described earlier, and aliquots were periodically withdrawn, blocked with AEMTS, and then desalted on a G25 column. Each sample was analyzed by cation-exchange HPLC. The same buffers were used here as in the purification of RNase B. A gradient of buffer B from

0 to 12% was applied from 20 to 120 min. A control experiment of RNase A was also carried out under the same conditions, using a slightly different gradient (from 3% to 14% buffer B) during the analysis in HPLC.

All peaks appearing in the HPLC chromatogram were collected separately and submitted for ESI/FTMS.

Top-Down MS Analysis for Mapping the Two Intermediates Obtained during the Reductive Unfolding of RNase B

In order to facilitate the mapping of the disulfide bonds in any reductive unfolding intermediate, the following procedure was used. At first, during the reductive unfolding process of RNase B, an aliquot of the aforementioned mixture at 15°C was quenched, 15 hr after its initiation, by the addition of glacial acetic acid (which brought the pH to 3 from pH 8). Since no AEMTS was added, a mixture with different species of proteins (native, unblocked intermediates, and unblocked-reduced protein) was obtained. The mixture was separated using a reversed-phase HPLC system, and peaks corresponding to various protein species were collected individually and lyophilized. In order to identify which unblocked species is a native protein, a reductive intermediate, or a fully reduced protein, a small amount of the lyophilized samples were blocked with AEMTS and introduced, individually, into the cation-exchange HPLC. By comparing the elution positions of the individual species with an AEMTS-blocked sample containing all species, it was possible to determine the nature (whether a native protein, reductive intermediate, or fully reduced protein) of each unblocked species on the reversed-phase system.

Once the peaks corresponding to the unblocked reductive intermediates on the reversed-phase system were identified, the intermediates were carboxymethylated with iodoacetamide (100 mM, pH 8, room temperature, 20 min in the dark). This procedure blocks only the free cysteines in the intermediates (these are the same free cysteines as those blocked with AEMTS during the reduction experiments). The carboxymethylated intermediates were desalted using reversed-phase HPLC and lyophilized. Finally, the carboxymethylated samples were fully reduced using DTT^{red} (100 mM, 100 mM Tris-HCl, 1 mM EDTA, pH 8) under strong denaturing conditions (6 M GdnHCl). The previously carboxymethylated cysteines were unaffected by this procedure, and only the remaining disulfides in each reductive intermediate were reduced; their corresponding free thiols were blocked with AEMTS. Reduced AEMTS-blocked carboxymethylated samples were desalted and lyophilized prior to MS analysis, as described earlier.

Acknowledgments

We thank H.J. Leung for collection of intermediates during the separation of the reductive unfolding mixture. We also thank Prof. A. Surolia for initiating our interest in RNase B and for suggestions about the preparation of this manuscript. This work was supported by the National Institute of General Medical Sciences of the National Institutes of Health (Grant Nos. GM-24893 and GM-16609). Support was also received from the National Foundation for Cancer Research.

Received: November 18, 2003
Revised: January 14, 2004
Accepted: January 21, 2004
Published: April 16, 2004

References

1. Rothman, J.E., and Lodish, H.F. (1977). Synchronised transmembrane insertion and glycosylation of a nascent membrane protein. Nature *269*, 775–780.
2. Joao, H.C., and Dwek, R.A. (1993). Effects of glycosylation on protein structure and dynamics in ribonuclease B and some of its individual glycoforms. Eur. J. Biochem. *218*, 239–244.
3. Arnold, U., and Ulbrich-Hofmann, R. (1997). Kinetic and thermodynamic thermal stabilities of ribonuclease A and ribonuclease B. Biochemistry *36*, 2166–2172.
4. Wormald, M.R., and Dwek, R.A. (1999). Glycoproteins: glycan presentation and protein-fold stability. Struct. Fold. Des. *7*, R155–R160.
5. Vijayan, M., and Chandra, N. (1999). Lectins. Curr. Opin. Struct. Biol. *9*, 707–714.
6. Molinari, M., and Helenius, A. (1999). Glycoproteins form mixed disulphides with oxidoreductases during folding in living cells. Nature *402*, 90–93.
7. Molinari, M., and Helenius, A. (2000). Chaperone selection during glycoprotein translocation into the endoplasmic reticulum. Science *288*, 331–333.
8. Kiely, M.L., McKnight, G.S., and Schimke, R.T. (1976). Studies on the attachment of carbohydrate to ovalbumin nascent chains in hen oviduct. J. Biol. Chem. *251*, 5490–5495.
9. Grafl, R., Lang, K., Vogl, H., and Schmid, F.X. (1987). The mechanism of folding of pancreatic ribonucleases is independent of the presence of covalently linked carbohydrate. J. Biol. Chem. *262*, 10624–10629.
10. Schülke, N., and Schmid, F.X. (1988). Effect of glycosylation on the mechanism of renaturation of invertase from yeast. J. Biol. Chem. *263*, 8832–8837.
11. Mathieu, M.E., Grigera, P.R., Helenius, A., and Wagner, R.R. (1996). Folding, unfolding, and refolding of the vesicular stomatitis virus glycoprotein. Biochemistry *35*, 4084–4093.
12. Nishimura, I., Uchida, M., Inohana, Y., Setoh, K., Daba, K., Nishimura, S., and Yamaguchi, H. (1998). Oxidative refolding of bovine pancreatic RNases A and B promoted by Asn-glycans. J. Biochem. (Tokyo) *123*, 516–520.
13. Tams, J.W., and Welinder, K.G. (1998). Glycosylation and thermodynamic versus kinetic stability of horseradish peroxidase. FEBS Lett. *421*, 234–236.
14. Reddy, G.B., Srinivas, V.R., Ahmad, N., and Surolia, A. (1999). Molten globule-like state of peanut lectin monomer retains its carbohydrate specificity — Implications in protein folding and legume lectin oligomerization. J. Biol. Chem. *274*, 4500–4503.
15. Bachhawat, K., Kapoor, M., Dam, T.K., and Surolia, A. (2001). The reversible two-state unfolding of a monocot mannose-binding lectin from garlic bulbs reveals the dominant role of the dimeric interface in its stabilization. Biochemistry *40*, 7291–7300.
16. Mitra, N., Sharon, N., and Surolia, A. (2003). Role of N-linked glycan in the unfolding pathway of erythrina corallodendron lectin. Biochemistry *42*, 12208–12216.
17. Sharon, N., and Lis, H. (1982). Glycoproteins. In The Proteins, Volume 5, H. Neurath and R.L. Hill, eds. (New York: Academic Press), pp. 1–144.
18. Goldenberg, D.P. (1988). Kinetic analysis of the folding and unfolding of a mutant form of bovine pancreatic trypsin inhibitor lacking the cysteine-14 and -38 thiols. Biochemistry *27*, 2481–2489.
19. Kuwajima, K., Ikeguchi, M., Sugawara, T., Hiraoka, Y., and Sugai, S. (1990). Kinetics of disulfide bond reduction in alpha-lactalbumin by dithiothreitol and molecular basis of superreactivity of the Cys6-Cys120 disulfide bond. Biochemistry *29*, 8240–8249.
20. Ewbank, J.J., and Creighton, T.E. (1993). Pathway of disulfide-coupled unfolding and refolding of bovine alpha-lactalbumin. Biochemistry *32*, 3677–3693.
21. Mendoza, J.A., Jarstfer, M.B., and Goldenberg, D.P. (1994). Effects of amino acid replacements on the reductive unfolding kinetics of pancreatic trypsin inhibitor. Biochemistry *33*, 1143–1148.
22. Li, Y.-J., Rothwarf, D.M., and Scheraga, H.A. (1995). Mechanism of reductive protein unfolding. Nat. Struct. Biol. *2*, 489–494.
23. Yamashita, H., Nakatsuka, T., and Hirose, M. (1995). Structural and functional characteristics of partially disulfide-reduced intermediates of ovotransferrin N lobe. Cystine localization by indirect end-labeling approach and implications for the reduction pathway. J. Biol. Chem. *270*, 29806–29812.
24. Ma, L.-C., and Anderson, S. (1997). Correlation between disulfide reduction and conformational unfolding in bovine pancreatic trypsin inhibitor. Biochemistry *36*, 3728–3736.
25. Chang, J.Y. (1997). A two-stage mechanism for the reductive unfolding of disulfide-containing proteins. J. Biol. Chem. *272*, 69–75.
26. Williams, R.L., Greene, S.M., and McPherson, A. (1987). The

crystal structure of ribonuclease B at 2.5 Å resolution. J. Biol. Chem. *262*, 16020–16031.
27. Fu, D., Chen, L., and O'Neill, R.A. (1994). A detailed structural characterization of ribonuclease B oligosaccharides by ^{1}H NMR spectroscopy and mass spectrometry. Carbohydr. Res. *261*, 173–186.
28. Rudd, P.M., Joao, H.C., Coghill, E., Fiten, P., Saunders, M.R., Opdenakker, G., and Dwek, R.A. (1994). Glycoforms modify the dynamic stability and functional activity of an enzyme. Biochemistry *33*, 17–22.
29. Wlodawer, A., Svensson, L.A., Sjölin, L., and Gilliland, G.L. (1988). Structure of phosphate-free ribonuclease A refined at 1.26 Å. Biochemistry *27*, 2705–2717.
30. Lyles, M.M., and Gilbert, H.F. (1991). Catalysis of the oxidative folding of ribonuclease A by protein disulfide isomerase: Dependence of the rate on the composition of the redox buffer. Biochemistry *30*, 613–619.
31. Rothwarf, D.M., and Scheraga, H.A. (1993). Regeneration of bovine pancreatic ribonuclease A. 1. Steady-state distribution. Biochemistry *32*, 2671–2679.
32. Udgaonkar, J.B., and Baldwin, R.L. (1995). Nature of the early folding intermediate of ribonuclease A. Biochemistry *34*, 4088–4096.
33. Ruoppolo, M., Torella, C., Kanda, F., Panico, M., Pucci, P., Marino, G., and Morris, H.R. (1996). Identification of disulphide bonds in the refolding of bovine pancreatic RNase A. Fold. Des. *1*, 381–390.
34. Rothwarf, D.M., Li, Y.-J., and Scheraga, H.A. (1998). Regeneration of bovine pancreatic ribonuclease A: identification of two nativelike three-disulfide intermediates involved in separate pathways. Biochemistry *37*, 3760–3766.
35. Rothwarf, D.M., Li, Y.-J., and Scheraga, H.A. (1998). Regeneration of bovine pancreatic ribonuclease A: detailed kinetic analysis of two independent folding pathways. Biochemistry *37*, 3767–3776.
36. Xu, X., Rothwarf, D.M., and Scheraga, H.A. (1996). Nonrandom distribution of the one-disulfide intermediates in the regeneration of ribonuclease A. Biochemistry *35*, 6406–6417.
37. Volles, M.J., Xu, X., and Scheraga, H.A. (1999). Distribution of disulfide bonds in the two-disulfide intermediates in the regeneration of bovine pancreatic ribonuclease A: further insights into the folding process. Biochemistry *38*, 7284–7293.
38. Pless, D.D., and Lennarz, W.J. (1977). Enzymatic conversion of proteins to glycoproteins. Proc. Natl. Acad. Sci. USA *74*, 134–138.
39. Puett, D. (1973). Conformational studies on a glycosylated bovine pancreatic ribonuclease. J. Biol. Chem. *248*, 3566–3572.
40. Joao, H.C., Scragg, I.G., and Dwek, R.A. (1992). Effects of glycosylation on protein conformation and amide proton exchange rates in RNase B. FEBS Lett. *307*, 343–346.
41. Cao, A., Welker, E., and Scheraga, H.A. (2001). Effect of mutation of proline 93 on redox unfolding/folding of bovine pancreatic ribonuclease A. Biochemistry *40*, 8536–8541.
42. Yang, Y., Wu, J., and Watson, J.T. (1999). Probing the folding pathways of long R^3 insulin-like growth factor-I (LR^3IGF-I) and IGF-I via capture and identification of disulfide intermediates by cyanylation methodology and mass spectrometry. J. Biol. Chem. *274*, 37598–37604.
43. Kelleher, N.L., Lin, H.Y., Valaskovic, G.A., Aaserud, D.J., Fridriksson, E.K., and McLafferty, F.W. (1999). Top down versus bottom up protein characterization by tandem high-resolution mass spectrometry. J. Am. Chem. Soc. *121*, 806–812.
44. Senko, M.W., Speir, J.P., and McLafferty, F.W. (1994). Collisional activation of large multiply charged ions using Fourier transform mass spectrometry. Anal. Chem. *66*, 2801–2808.
45. Horn, D.M., Zubarev, R.A., and McLafferty, F.W. (2000). Automated reduction and interpretation of high resolution electrospray mass spectra of large molecules. J. Am. Soc. Mass Spectrom. *11*, 320–332.
46. Ge, Y., Lawhorn, B.G., ElNaggar, M., Strauss, E., Park, J.-H., Begley, T.P., and McLafferty, F.W. (2002). Top down characterization of large proteins (45 KDa) by electron capture dissociation mass spectrometry. J. Am. Chem. Soc. *124*, 672–678.
47. Beu, S.C., Senko, M.W., Quinn, J.P., and McLafferty, F.W. (1993). Improved Fourier-transform ion-cyclotron-resonance mass spectrometry of large biomolecules. J. Am. Soc. Mass Spectrom. *4*, 190–192.
48. Thannhauser, T.W., and Scheraga, H.A. (1985). Reversible blocking of half-cystine residues of proteins and an irreversible specific deamidation of asparagine-67 of S-sulforibonuclease under mild conditions. Biochemistry *24*, 7681–7688.